Published in final edited form as:
J Immunol. 2014 March 15; 192(6): 2622–2633. doi:10.4049/jimmunol.1301369.

Pan-Bcl-2 Inhibitor, GX15-070 (Obatoclax), Decreases Human T Regulatory Lymphocytes While Preserving Effector T Lymphocytes: a Rationale for Its Use in Combination Immunotherapy

Peter S. Kim, **Caroline Jochems**, **Italia Grenga**, **Renee N. Donahue**, **Kwong Y. Tsang**, **James L. Gulley**, **Jeffrey Schlom***, and **Benedetto Farsaci***
Laboratory of Tumor Immunology and Biology, Center for Cancer Research, National Cancer Institute, National Institutes of Health, Bethesda, MD, 20892

Abstract

Bcl-2 inhibitors are currently being evaluated in clinical studies for treatment of patients with solid tumors and hematopoietic malignancies. In this study we explored the potential for combining the pan-Bcl-2 inhibitor GX15-070 (GX15; obatoclax) with immunotherapeutic modalities. We evaluated the *in vitro* effects of GX15 on human T-cell subsets obtained from PBMCs in terms of activation, memory, and suppressive function. Our results indicated that in healthy-donor PBMCs, mature-activated T cells were more resistant to GX15 than early-activated T cells, and that GX15 preserved memory but not non-memory T-cell populations. Furthermore, GX15 increased the apoptosis of regulatory T cells (Tregs), profoundly down-regulated FOXP3 and CTLA-4 in a dose-dependent manner, and decreased their suppressive function. Treating PBMCs obtained from ovarian cancer patients with GX15 also resulted in increased $CD8^+$:Treg and $CD4^+$:Treg ratios. These results support preclinical studies in which mice vaccinated before treatment with GX15 showed the greatest reduction in metastatic lung tumors as a result of increased apoptotic resistance of mature $CD8^+$ T cells and decreased Treg function brought about by GX15. Taken together, these findings suggest that when a Bcl-2 inhibitor is combined with active immunotherapy in humans, such as the use of a vaccine or immune checkpoint inhibitor, immunotherapy should precede administration of the Bcl-2 inhibitor to allow T cells to become mature, and thus resistant to the cytotoxic effects of the Bcl-2 inhibitor.

Introduction

GX15-070 (GX15; obatoclax), a pan-Bcl-2 inhibitor, has been widely tested in clinical trials ever since the U.S. Food and Drug Administration granted it orphan drug status for the treatment of chronic lymphocytic leukemia. GX15 has also been tested preclinically and clinically for efficacy in acute myelogenous leukemia (1), mantle cell lymphoma (2),

Address correspondence and reprint requests to Jeffrey Schlom, Laboratory of Tumor Immunology and Biology, Center for Cancer Research, National Cancer Institute, National Institutes of Health, 10 Center Drive, Room 8B09, Bethesda, MD 20892. Tel: 301-496-4343; fax: 301-496-2756, js141c@nih.gov.
*Both authors contributed equally

multiple myeloma (3), myelofibrosis (4), and solid tumors such as small-cell lung cancer (5–9).

GX15 is a synthetic derivative of bacterial prodiginines belonging to the polypyrrole class of molecules. GX15 mimics the BH3 domain of the antiapoptotic family members of Bcl-2, but differs from other Bcl-2 inhibitors by having consistent binding properties across all antiapoptotic Bcl-2 family members, including Bcl-2, Bcl-xL, Bcl-w, Mcl-1, and Bak, and is thus classified as a pan-Bcl-2 inhibitor. For instance, other Bcl-2 inhibitors such as ABT-737 and ABT-263 have higher binding affinity to Bcl-2 and Bcl-xL than does GX15, but they do not bind to all Bcl-2 family members (most notably, not to Mcl-1) (10, 11). Therefore, tumor cells may become resistant to ABT-737 and ABT-263 by overexpression of Mcl-1, which GX15 has been shown to inhibit (12).

In preclinical studies, a wide range of GX15 concentrations was used depending on the targets to be assayed. For instance, IC_{50} values of GX15 in human lung cancer cell lines ranged from 1.33 μM to 15.4 μM (8). In clinical studies, C_{max} of GX15 was reported to be in the range of 0.03 to 0.36 μM (11). In a phase I dose-escalation study of GX15 in patients with advanced solid tumors or lymphoma, the maximum tolerated dose using a 3-hour i.v. infusion schedule in 27 patients was 20 mg/m^2, with C_{max} of 0.28 μM and AUC of 0.95 μM (5). Based on *in vitro* concentrations of GX15 and pharmacokinetic data derived from a search of the literature, we used GX15 in concentrations ranging from 0.1 μM to 5 μM. As a single agent, GX15 has thus far shown modest clinical activity (10, 11), leading some investigators to combine GX15 with other anticancer agents such as bortezomib (a proteasome inhibitor) (13, 14) and SNDX-275 (a histone deacetylase inhibitor) (15–17). These combinations have had an enhanced antitumor effect against hematologic malignancies.

In a preclinical model, we previously investigated the potential of GX15 to synergize with vaccine-based immunotherapy using a recombinant vaccine (recombinant vaccinia (rV-); recombinant fowlpox (rF-)) encoding the tumor-associated carcinoembryonic antigen (CEA) and a TRIad of COstimulatory Molecules (rV/F-CEA-TRICOM) in CEA-transgenic mice (18). We determined that the sensitivity of murine lymphocytes to GX15 was dependent on their activation status, as mature-activated CD69$^-$ lymphocytes were more resistant to GX15 than early-activated CD69$^+$ lymphocytes *in vitro* (18). This finding suggested that GX15 should ideally be administered after lymphocytes have undergone full maturation post-vaccination (18). In addition, GX15 impaired the suppressive function of murine regulatory T cells (Tregs) isolated from GX15-treated mice (18). Finally, sequential combination therapy with rV/F-CEA-TRICOM vaccine followed by GX15 effectively reduced orthotopic pulmonary tumors (18), providing a rationale for designing similar combination protocols for clinical trials.

In this study, we evaluated the effect of GX15 on specific subsets of human T lymphocytes. Using PBMCs from healthy donors and ovarian cancer patients, GX15 toxicity depended on the activation status of human T lymphocytes, as indicated by CD69 expression. Furthermore, GX15 down-regulated expression levels of both FOXP3 and CTLA-4 in human Tregs and decreased their suppressive function. The data obtained from this study

provide a further rationale for the clinical translation of the combination of active immunotherapy agents in a temporal regimen with the Bcl-2 inhibitor GX15.

Materials and Methods

Drug preparation

GX15 (obatoclax) was obtained through an agreement between the Cancer Therapeutic Evaluation Program of the National Cancer Institute and Teva Pharmaceuticals (Petah Tikva, Israel). The GX15 was dissolved in DMSO at a concentration of 200 mM. For treatment of human PBMCs or isolated $CD8^+$ T cells, 200 mM of GX15 was diluted accordingly and added at 1 μL per 10^6 cells/mL at final concentrations ranging from 0.1 to 5 μM.

Isolation of regulatory T cells

Regulatory T cells were isolated from PBMCs from healthy donors using a $CD4^+/CD25^+/CD127^{dim/-}$ Regulatory T Cell Isolation Kit II (Miltenyi) according to the manufacturer's protocol.

Proliferation analysis

CellTrace™ Violet (CTV) Cell Proliferation Kit (Molecular Probes Inc., Eugene, OR) was used, with some modifications, to label T lymphocytes. First we prepared a cell suspension of 10^7 cells/mL and a 5-mM stock solution of CTV, then added 0.2 μL of the 5-mM CTV stock solution per 1 mL of the cell suspension for a final working concentration of 1 μM. CTV-containing cells were incubated at 37°C in the dark for 10 min. The reaction was stopped by adding 5X volume of cold medium and incubating on ice for 5 min. Cells were spun, resuspended in a prewarmed medium, and incubated at 37°C in the dark for at least 10 min to facilitate acetate hydrolysis.

Early and prolonged activation of T lymphocytes

For early activation of T lymphocytes, 24-well plates were coated with 750 μL of anti-CD3 (Clone: UCHT1; BD Biosciences, San Jose, CA) at 0.5 μg/mL in PBS and then kept at 4°C. Cryopreserved PBMCs from healthy donors were thawed and rested at 37°C with 5% CO_2 overnight prior to stimulation. For resting, PBMCs at 1×10^6 cells/mL in IMDM containing 10% human serum were added 5 mL per well (5×10^6 PBMCs/well) in 6-well plates overnight at 37°C, 5% CO_2. After resting overnight, non-adherent cells were first collected and then combined with adherent cells, which were gently removed with a cell scraper. PBMCs were then prepared at 1×10^6 cells/mL, followed by the addition of soluble anti-CD28 antibody (Clone: CD28.2; BD Biosciences) at a final concentration of 0.5 μg/mL. Anti-CD3-coated plates were washed once with 1 mL PBS, and 1 mL (1×10^6 cells) of the anti-CD28-containing cell suspension in a medium containing IL-7 and IL-15 (Peprotech, Rocky Hill, NJ) at 10 ng/mL for each cytokine was added to each well of the anti-CD3-coated plates. Cells were stimulated for 3 days. For prolonged activation, early-activated cells were transferred to 6-well plates at 1×10^6 cells/mL (total 3 mL/well) in IL-7/IL-15 containing medium on day 3. Cells were replenished with IL-7 and IL-15 with 3 mL of IL-7/IL-15-containing medium/well on day 5. On day 7, cells were harvested, labeled using a

CellTrace™ Violet Cell Proliferation Kit, then replated in 24-well plates at 1×10^6 cells/mL (total 1 mL/well) in fresh IL-7/IL-15 medium. On day 9, cells were replenished with 1 mL of the IL-7/IL-15 medium.

Expansion of Tregs

Isolated Tregs were expanded using a Treg Expansion Kit (Miltenyi) according to the manufacturer's protocol. Tregs were activated with CD3/CD28 MACSi Beads (Miltenyi) for 1 d, then supplemented with IL-2 (Peprotech) at 500 U/mL during the 14-d expansion period.

Treg suppression assay

Tregs were first pre-treated with GX15 at 1 μM for 24 h. $CD4^+CD25^-$ Teff cells (1×10^4 cells/mL) were cultured alone or cocultured with Tregs (1×10^4, 5×10^3, or 1×10^3 cells/mL) with 1 μg/mL of plate-bound anti-CD3 (clone OKT3: eBioscience, San Diego, CA) and irradiated (3,500 rad) T cell-depleted PBMCs (1×10^5 cells/mL) in a 96-well flat-bottom plate at 37°C and 5% CO_2. On day 4, T-cell proliferation was measured by [3H]thymidine (PerkinElmer, Waltham, MA) incorporation at 1μCi (0.037 MBq)/well and quantified 16 h later using a Wizard 2 gamma counter. Proliferation of $CD4^+CD25^-$ T cells without Tregs was defined as 100% proliferation. Percent suppression was calculated using the following formula: (cpm of Teff cells alone – cpm of Teff cells treated with Treg)/cpm of Teff cells alone).

In vitro treatment with GX15

GX15 at a concentration of 5 μM was used for early and prolonged activation studies of PBMCs from healthy donors (n = 3). GX15 at a concentration of 1 μM was used for Treg suppression assay. GX15 at concentrations of 0.1, 1.0, and 5.0 μM was used to treat expanded Tregs and PBMCs taken from stage IIIc or IV ovarian cancer patients (n = 4) who had progressed on chemotherapy. All samples were obtained prior to experimental therapy but after enrollment on a National Cancer Institute Institutional Review Board approved clinical trial (NCT00088413). Equivalent concentrations of DMSO were used as controls in each study.

Flow cytometry analysis; surface and intracellular marker assays

An LSR-II flow cytometer (BD Biosciences) was used for multiparametric flow cytometry analysis. Because GX15 emits a red color, photomultiplier tube settings had to be adjusted, in particular the FITC and PE channels, and appropriate isotype controls or fluorescence minus one controls were used for gating at each GX15 concentration. A Live/Dead® Fixable Blue Dead Cell Stain Kit (Molecular Probes Inc.) was used to exclude dead cells. The following human mAbs were used to stain PBMCs from healthy donors: FITC-CD45RA, PerCP-Cy5.5 Annexin V, and V500-CD3 (BD Biosciences), PE-Cy7-CD69, APC-CD4, and AF700-CD8 (eBioscience). The following human mAbs were used to stain enriched and expanded Tregs: V500-CD3, Alexa Fluor 647-cleaved PARP (Poly (ADP-ribose) polymerase), PE-CD127, PerCP-Cy5.5 Annexin V, APC-Cy7-CD25 (BD Biosciences), Alexa Fluor 700-CD4, and PE-Cy7-FOXP3 (eBioscience). The following mAbs were used

to stain PBMCs from ovarian cancer patients: FITC-CD45RA, PerCP-Cy5.5-Annexin V, APC-Cy7-CD25 (BD Biosciences), PE-CD4, APC-CTLA-4, Brilliant Violet 510-CD8, Brilliant Violet 421-CD69, Brilliant Violet 605-CD127 (BioLegend, San Diego, CA), and PE-Cy7-FOXP3 (eBioscience). A FOXP3/Transcription Factor Staining Buffer set (eBioscience) was used for intracellular staining of FOXP3, CTLA-4, and cleaved PARP.

Statistical analysis

Unless specified, results of tests of significance are indicated as *p* values, derived from a 2-tailed Mann-Whitney test. All *p* values were derived at 95% using GraphPad Prism 6® statistical software for PCs.

Results

Prolonged activation made enriched CD8$^+$ T cells from healthy-donor PBMCs more resistant to GX15 than early-activated CD8$^+$ T cells

We first evaluated the extent to which GX15 affects human CD4$^+$ and CD8$^+$ T cells from healthy-donor PBMCs (n = 3) after early or prolonged activation (Fig. 1). To test early activation, PBMCs were stimulated with anti-CD3 and anti-CD28 in the presence of IL-7 and IL-15 for 3 days, then treated with GX15 for 24 h at 5 μM (Fig. 1A). To test prolonged activation, PBMCs that had been stimulated for 3 days were maintained in culture with IL-7 and IL-15 for an additional 7 days, then treated with GX15 for 24 hrs at 5 μM (Fig. 1A). Results showed that GX15 significantly decreased the number and viability of PBMCs after early activation, but had no significant effect after prolonged activation (Fig. 1B). To determine the effect of GX15 on early- and prolonged-activated CD4$^+$ and CD8$^+$ T cells, we performed a flow analysis to measure the level of cleaved PARP. in live GX15-treated T cells (Fig. 1B). Results showed that there was a greater increase in apoptosis, as measured by the expression level of cleaved PARP, in both early-activated CD4$^+$ and CD8$^+$ T cells compared to their prolonged-activated counterparts after GX15 treatment (Fig. 1B). Thus, CD4$^+$ and CD8$^+$ T cells that had been activated and then maintained in culture were more resistant to GX15 compared to early-activated CD4$^+$ and CD8$^+$ T cells.

Early-activated (CD69$^+$) T cells from healthy-donor PBMCs were more sensitive to GX15 compared to prolonged-activated (CD69$^-$) T cells

We next examined whether expression of the early-activation marker CD69 on human CD4$^+$ and CD8$^+$ T cells made the cells more sensitive to GX15 after early and prolonged activation (Fig. 2). We analyzed nonapoptotic (cleaved PARP$^-$ and annexin V$^-$) cells taken from PBMCs of 3 additional healthy donors who had undergone either early or prolonged activation *in vitro* (Fig. 2). Results showed that GX15 at 5 μM decreased CD69 expression to a greater extent in early-activated CD4$^+$ (2 of 3 donors) and CD8$^+$ T cells (all donors) than in prolonged-activated CD4$^+$ and CD8$^+$ T cells (Fig. 2). This suggested that CD69$^+$ T cells are more sensitive to GX15 than CD69$^-$ T cells, especially after early activation (Fig. 3). We then examined the effect of GX15 on T-cell proliferation based on CD69 expression. GX15 had a greater inhibitory effect on the highly proliferating (Generation 3) CD4$^+$/CD69$^+$ (all donors) and CD8$^+$/CD69$^+$ (2 of 3 donors) populations after early activation than after

prolonged activation (Fig. 3). In addition, GX15 had no effect on the proliferation of the $CD69^-$ population after prolonged activation, most notably in $CD8^+$ T cells (Fig. 3).

Nonmemory ($CD45RA^+$) T cells were more sensitive to GX15 than memory ($CD45RA^-$) T cells

Our results showed that the activation status of T cells, based on CD69 expression, can determine T-cell sensitivity to GX15. Because Bcl-2 has been shown to play a dynamic role in T-cell differentiation, memory formation, and survival (19–22), we explored the extent to which the memory status of T cells is affected by treatment with GX15 after early and prolonged activation (Fig. 4). Treatment with 5 μM of GX15 resulted in a significant decrease in the proportion of nonmemory ($CD45RA^+$) $CD4^+$ and $CD8^+$ T cells after early activation in all donors, while the proportion of memory ($CD45RA^-$) T cells was preserved (Fig. 4). In prolonged activation, 5 μM of GX15 resulted in a decrease in $CD4^+$ $CD45RA^+$ cells in 1 of 3 donors, whereas $CD8^+$ $CD45RA^+$ cells decreased in all donors (Fig. 4). As with CD69 expression, we also examined the effect of GX15 on T-cell proliferation based on CD45RA expression. Results showed that GX15 greatly inhibited the highly proliferating (Generation 3) $CD45RA^+$ and $CD45RA^-$ cells in both $CD4^+$ and $CD8^+$ T-cell populations after early activation (Fig. 5). With prolonged activation, $CD45RA^-$ proliferation was notably maintained in the $CD8^+$ T-cell population (Fig. 5).

Treatment with GX15 resulted in apoptosis and down-regulation of FOXP3 in Tregs

To study the effect of GX15 on Tregs from human PBMCs, we first isolated and then expanded human Tregs from healthy-donor PBMCs (Fig. 6A). We determined the purity of isolated and expanded human Tregs by flow cytometry analysis and gating of live $CD4^+$, $CD25^+$, $FOXP3^+$, and $CD127^-$ cells (Fig. 6B). Activation of T cells has been shown to expose phosphatidylserine on the cell surface (23, 24), which may confound the results derived from annexin V-based measurements of apoptotic cells. Therefore, we measured the level of apoptosis induced by GX15 in Tregs by cleaved PARP expression on live annexin V^- cells (Fig. 6C). We also examined the level of FOXP3 expression in Tregs treated with GX15, since other studies have shown that the mean fluorescence intensity (MFI) of FOXP3 positively correlates with Treg function (25–27). Our results showed that GX15 at 0.1, 1, and 5 μM for 24 h increased cleaved PARP expression in Tregs (Fig. 6D). More interestingly, GX15 treatment noticeably down-regulated expression of FOXP3, suggesting that GX15 may potentially impair Treg function (Fig. 6D).

Tregs were more sensitive to GX15 than $CD4^+$ effector T cells

To determine whether Tregs and effector T cells have different sensitivity to GX15, we analyzed the effect of GX15 on PBMCs from several cancer patients. PBMCs from ovarian cancer patients (n = 4) were thawed, and then rested for 24 h before treatment with GX15 at 0.1, 1.0, and 5.0 μM (Fig. 7A). Results indicated that Tregs were significantly more sensitive than $CD4^+$ T cells to GX15 at 1.0 and 5.0 μM (Fig. 7B). Furthermore, Tregs expressed a significantly higher level of the early-activation marker $CD69^+$ compared to $CD4^+$ T cells, which could explain the higher sensitivity of Tregs to GX15 compared to $CD4^+$ T cells (Fig. 7C). In addition, at 1.0 μM GX15 down-regulated FOXP3 in Tregs from all 4 patient samples and further decreased FOXP3 expression at 5.0 μM (Fig. 7D). CTLA-4 expression

in Tregs also decreased after treatment with 0.1 μM of GX15, and decreased further in a dose-dependent manner at 1.0 and 5.0 μM (Fig. 7D). Taken together, these findings show not only that Tregs are more sensitive than $CD4^+$ T cells to GX15, but also that GX15 treatment likely impairs the functional capacity of Tregs.

Treatment with GX15 resulted in functional impairment of Tregs

Isolated Tregs from healthy-donor PBMCs were tested for their suppressive function after treatment with GX15. We used a 1 μM concentration of GX15 rather than a 5 μM concentration because it more effectively maintained the viability of Tregs (Fig. 8B). In addition, down-regulation of FOXP3 with 1 μM of GX15 (Fig. 8C) was comparable to that of 5 μM of GX15 (Fig. 8C) and significantly decreased CTLA-4 expression in Tregs undergoing apoptosis (Fig. 8C). Results also showed that 1 μM of GX15 reduced the suppressive function of Tregs in all 3 donors (Fig. 8D).

Ratios of both $CD4^+$ and $CD8^+$ T cells to Tregs increased after GX15 treatment

Because Tregs are more sensitive than $CD4^+$ T cells to GX15 (Fig. 7B), we analyzed the extent to which GX15 treatment altered the ratio of $CD4^+$ or $CD8^+$ T cells to Tregs in PBMCs from cancer patients (Fig. 9A). Our results showed that GX15 at 5.0 μM significantly increased the ratio of $CD4^+$ and $CD8^+$ T cells to Tregs in 3 of 4 PBMC samples (Fig. 9B).

Discussion

Because improved tumor control would likely require combining GX15 with another anticancer modality, we decided to examine the potential of GX15 in combination with immunotherapy by analyzing the effects of GX15 on human T lymphocytes. Specifically, we focused on measuring the *in vitro* sensitivity of differently activated T lymphocytes to the pan-Bcl-2 inhibitor. We also studied the effects of GX15 *in vitro* treatment on Tregs and on the balance of effector vs. suppressor immune elements in the PBMCs of cancer patients. This study follows a preclinical investigation in mice that tested the use of the tumor antigen-specific vaccine rV/F-CEA-TRICOM in an orthotopic pulmonary tumor model (18). From this mouse study, we determined that GX15 did not affect mature-activated $CD8^+$/$CD69^-$ T cells, but did decrease the suppressive function of Tregs, thereby enhancing the vaccine-mediated antitumor efficacy of rV/F-CEA-TRICOM in a Lewis lung tumor model (18). Based on these results, the timing of GX15 administration was determined to be critical, and that an immunotherapeutic regimen should precede GX15 treatment to achieve optimal antitumor effects.

Initially, we determined that human T lymphocytes were more sensitive to GX15 after early activation than prolonged activation (Fig. 1B). This result was consistent with our preclinical study (18), which found that GX15 should be administered long enough after vaccination to allow activated $CD8^+$ T lymphocytes to undergo sufficient maturation and become resistant to the Bcl-2 inhibitor. We thus determined that sequential treatment with vaccine followed by GX15 would be more immune-favorable than coadministration of both agents or GX15 treatment followed by vaccine.

We further investigated the effect of GX15 on human T-lymphocyte subsets after early and prolonged activation, based on their activation, memory, and suppressive function. Ideally, testing a large number of PBMC samples from cancer patients would have been most appropriate. However, due to the scarcity of patient samples available for this study, we felt the best alternative was to use PBMCs from healthy donors. We found that after early and prolonged activation, $CD4^+$ and $CD8^+$ T cells (obtained from PBMCs of healthy donors) that expressed the early-activation marker CD69 were sensitive to GX15 (Fig. 2), which corresponded with data from the mouse study (18). An underlying mechanism for the greater sensitivity of human $CD69^+$ T cells to GX15 could be increased expression of the myeloid-cell leukemia differentiation protein-1 (Mcl-1) induced during early activation of T cells. It has been shown that human T cells upregulate the Mcl-1 gene within 10 h after T-cell receptor ligation, suggesting a role for Mcl-1 in early activation (28). In addition, GX15 noticeably decreased highly proliferating cells in the $CD69^+$ T-cell population but had less of an effect on low-proliferating $CD69^+$ T cells (Fig. 3), suggesting that GX15 has a cytostatic effect (1, 29). In contrast, GX15 altered the proliferation of $CD69^-$ T cells to a lesser degree than $CD69^+$ T cells, most notably in prolonged activation (Fig. 3).

It has been shown that Bcl-2 sends signals necessary for the survival and maintenance of memory cells by way of the gamma-chain cytokines IL-7 and IL-15 (30, 31). For this reason, we examined the effect of GX15 on human memory T cells after prolonged activation upon IL-7/IL-15 *in vitro* maintenance (Figs. 4 and 5). We found that GX15 treatment consistently decreased the nonmemory compartment ($CD45RA^+$) of the $CD8^+$ T cell population in healthy-donor PBMCs, whereas the memory compartment ($CD45RA^-$) was unaffected (Fig. 4). Just as Bcl-2 in memory T cells was shown to tolerate higher expression of the pro-apoptotic molecule Bim (19), it is likely that after prolonged activation, memory T cells in our study were better able to tolerate GX15 than nonmemory ($CD45RA^+$) cells *in vitro* due to stable maintenance of Bcl-2 expression induced by exogenous administration of IL-7 and IL-15.

We had previously determined that GX15 significantly reduced Treg function and increased the $CD8^+$:Treg ratio in tumor-bearing mice (18). Based on this finding, we investigated whether similar results would be seen in PBMCs from cancer patients. Our most striking finding was the degree to which cancer patients' Treg numbers were reduced after treatment with GX15, compared to effector $CD4^+$ T cells from cancer patients (Fig. 7B). We believe that one of the reasons for Tregs' higher sensitivity to GX15 is their higher CD69 expression compared to non-Treg $CD4^+$ T cells (Fig. 7C), which indicates a higher proportion of early-activated Tregs compared to $CD4^+$ T cells in the PBMCs of cancer patients. Furthermore, expression of FOXP3 and CTLA-4 in Tregs from PBMCs of cancer patients decreased in a dose-dependent manner after treatment with GX15 (Fig. 7D). It is worth noting that CTLA-4 expression in Tregs began to decrease at a GX15 concentration of 0.1 μM, which is within the range of C_{max} reported in clinical studies (5, 32). Overall, these results suggest Treg functional impairment, as various studies have shown an inverse correlation between FOXP3 or CTLA-4 expression and Treg functionality (25–27, 33–35). Furthermore, when Tregs were treated with GX15, their suppressive activity was shown to be reduced (Fig. 8D). This, plus the finding that GX15 treatment increased the $CD4^+$:Treg and $CD8^+$:Treg ratios

(Fig. 9), leads us to believe that GX15 treatment may numerically favor nonregulatory $CD4^+$ and $CD8^+$ T cells and concomitantly reduce Treg function in the clinical setting.

Data obtained from this study may have implications for the clinical use of GX15 in combination with an active immunotherapeutic platform such as a vaccine or immune checkpoint inhibitors. The schedule of administration of each agent is potentially important, since immunotherapy-induced immunity may decrease if the period between immunization and GX15 treatment is too short. For optimum effect, an immune-stimulating agent directed at T cells should precede GX15 treatment long enough for activated T cells to fully mature and acquire resistance to GX15. Proper treatment scheduling will also maintain viable memory T cells, thereby establishing a sustainable source of cytotoxic T cells that can attack tumors. Because human Tregs are sensitive to GX15, the pan-Bcl-2 inhibitor could potentially tip the numerical and functional balance of effector T cells and Tregs toward effector T cells in the human tumor microenvironment. The model shown in this study could be extended to other Bcl-2 inhibitors such as ABT-737 and its orally active analog ABT-263 for sequential combination immunotherapy, as discussed above. However, because these agents do not inhibit Mcl-1, it is possible that tumors may develop Mcl-1-mediated resistance to ABT-737 or ABT-263. In this context, it may be necessary to coadminister an agent that inhibits or down-regulates Mcl-1 (36–39) along with ABT-737 or ABT-263 to provide comparable inhibition of Bcl-2 family molecules such as GX15.

To our knowledge, this is the first study to examine the effect of a Bcl-2 inhibitor on human T cells based on their activation, memory, and suppressive status. This study may provide a rationale for sequentially combining Bcl-2 inhibitors with a checkpoint inhibitor or vaccine-based immunotherapy in a clinical setting.

Acknowledgments

This research was supported by the Intramural Research Program of the Center for Cancer Research, National Cancer Institute, National Institutes of Health

The authors acknowledge the excellent editorial assistance of Bonnie L. Casey and Debra Weingarten in the preparation of this manuscript.

Abbreviations used in this article

CEA	carcinoembryonic antigen
CTV	CellTrace™ Violet
MFI	mean fluorescence intensity
PARP	Poly (ADP-ribose) polymerase
Teff	effector T cells
Tregs	regulatory T cells
TRICOM	TRIad of COstimulatory Molecules

References

1. Konopleva M, Watt J, Contractor R, Tsao T, Harris D, Estrov Z, Bornmann W, Kantarjian H, Viallet J, Samudio I, Andreeff M. Mechanisms of antileukemic activity of the novel Bcl-2 homology domain-3 mimetic GX15-070 (obatoclax). Cancer Res. 2008; 68:3413–3420. [PubMed: 18451169]
2. Campas C, Cosialls AM, Barragan M, Iglesias-Serret D, Santidrian AF, Coll-Mulet L, de Frias M, Domingo A, Pons G, Gil J. Bcl-2 inhibitors induce apoptosis in chronic lymphocytic leukemia cells. Exp Hematol. 2006; 34:1663–1669. [PubMed: 17157163]
3. Trudel S, Li ZH, Rauw J, Tiedemann RE, Wen XY, Stewart AK. Preclinical studies of the pan-Bcl inhibitor obatoclax (GX015-070) in multiple myeloma. Blood. 2007; 109:5430–5438. [PubMed: 17332241]
4. Parikh SA, Kantarjian H, Schimmer A, Walsh W, Asatiani E, El-Shami K, Winton E, Verstovsek S. Phase II study of obatoclax mesylate (GX15-070), a small-molecule BCL-2 family antagonist, for patients with myelofibrosis. Clin Lymphoma Myeloma Leuk. 2010; 10:285–289. [PubMed: 20709666]
5. Hwang JJ, Kuruvilla J, Mendelson D, Pishvaian MJ, Deeken JF, Siu LL, Berger MS, Viallet J, Marshall JL. Phase I dose finding studies of obatoclax (GX15-070), a small molecule pan-BCL-2 family antagonist, in patients with advanced solid tumors or lymphoma. Clin Cancer Res. 2010; 16:4038–4045. [PubMed: 20538761]
6. Paik PK, Rudin CM, Brown A, Rizvi NA, Takebe N, Travis W, James L, Ginsberg MS, Juergens R, Markus S, Tyson L, Subzwari S, Kris MG, Krug LM. A phase I study of obatoclax mesylate, a Bcl-2 antagonist, plus topotecan in solid tumor malignancies. Cancer Chemother Pharmacol. 2010; 66:1079–1085. [PubMed: 20165849]
7. Chiappori AA, Schreeder MT, Moezi MM, Stephenson JJ, Blakely J, Salgia R, Chu QS, Ross HJ, Subramaniam DS, Schnyder J, Berger MS. A phase I trial of pan-Bcl-2 antagonist obatoclax administered as a 3-h or a 24-h infusion in combination with carboplatin and etoposide in patients with extensive-stage small cell lung cancer. Br J Cancer. 2012; 106:839–845. [PubMed: 22333598]
8. Li J, Viallet J, Haura EB. A small molecule pan-Bcl-2 family inhibitor, GX15-070, induces apoptosis and enhances cisplatin-induced apoptosis in non-small cell lung cancer cells. Cancer Chemother Pharmacol. 2008; 61:525–534. [PubMed: 17505826]
9. Paik PK, Rudin CM, Pietanza MC, Brown A, Rizvi NA, Takebe N, Travis W, James L, Ginsberg MS, Juergens R, Markus S, Tyson L, Subzwari S, Kris MG, Krug LM. A phase II study of obatoclax mesylate, a Bcl-2 antagonist, plus topotecan in relapsed small cell lung cancer. Lung Cancer. 2011; 74:481–485. [PubMed: 21620511]
10. Goard CA, Schimmer AD. An evidence-based review of obatoclax mesylate in the treatment of hematological malignancies. Core Evid. 2013; 8:15–26. [PubMed: 23515850]
11. Joudeh J, Claxton D. Obatoclax mesylate: pharmacology and potential for therapy of hematological neoplasms. Expert Opin Investig Drugs. 2012; 21:363–373.
12. Nguyen M, Marcellus RC, Roulston A, Watson M, Serfass L, Murthy Madiraju SR, Goulet D, Viallet J, Belec L, Billot X, Acoca S, Purisima E, Wiegmans A, Cluse L, Johnstone RW, Beauparlant P, Shore GC. Small molecule obatoclax (GX15-070) antagonizes MCL-1 and overcomes MCL-1-mediated resistance to apoptosis. Proc Natl Acad Sci U S A. 2007; 104:19512–19517. [PubMed: 18040043]
13. Perez-Galan P, Roue G, Lopez-Guerra M, Nguyen M, Villamor N, Montserrat E, Shore GC, Campo E, Colomer D. BCL-2 phosphorylation modulates sensitivity to the BH3 mimetic GX15-070 (obatoclax) and reduces its synergistic interaction with bortezomib in chronic lymphocytic leukemia cells. Leukemia. 2008; 22:1712–1720. [PubMed: 18596739]
14. Perez-Galan P, Roue G, Villamor N, Campo E, Colomer D. The BH3-mimetic GX15-070 synergizes with bortezomib in mantle cell lymphoma by enhancing Noxa-mediated activation of Bak. Blood. 2007; 109:4441–4449. [PubMed: 17227835]
15. Wei Y, Kadia T, Tong W, Zhang M, Jia Y, Yang H, Hu Y, Tambaro FP, Viallet J, O'Brien S, Garcia-Manero G. The combination of a histone deacetylase inhibitor with the Bcl-2 homology domain-3 mimetic GX15-070 has synergistic antileukemia activity by activating both apoptosis and autophagy. Clin Cancer Res. 2010; 16:3923–3932. [PubMed: 20538760]

16. Jona A, Khaskhely N, Buglio D, Shafer JA, Derenzini E, Bollard CM, Medeiros LJ, Illes A, Ji Y, Younes A. The histone deacetylase inhibitor entinostat (SNDX-275) induces apoptosis in Hodgkin lymphoma cells and synergizes with Bcl-2 family inhibitors. Exp Hematol. 2011; 39:1007–1017. e1001. [PubMed: 21767511]
17. Wei Y, Kadia T, Tong W, Zhang M, Jia Y, Yang H, Hu Y, Viallet J, O'Brien S, Garcia-Manero G. The combination of a histone deacetylase inhibitor with the BH3-mimetic GX15-070 has synergistic antileukemia activity by activating both apoptosis and autophagy. Autophagy. 2010; 6:976–978. [PubMed: 20729640]
18. Farsaci B, Sabzevari H, Higgins JP, Di Bari MG, Takai S, Schlom J, Hodge JW. Effect of a small molecule BCL-2 inhibitor on immune function and use with a recombinant vaccine. Int J Cancer. 2010; 127:1603–1613. [PubMed: 20091862]
19. Wojciechowski S, Tripathi P, Bourdeau T, Acero L, Grimes HL, Katz JD, Finkelman FD, Hildeman DA. Bim/Bcl-2 balance is critical for maintaining naive and memory T cell homeostasis. J Exp Med. 2007; 204:1665–1675. [PubMed: 17591857]
20. Kurtulus S, Tripathi P, Moreno-Fernandez ME, Sholl A, Katz JD, Grimes HL, Hildeman DA. Bcl-2 allows effector and memory CD8+ T cells to tolerate higher expression of Bim. J Immunol. 2011; 186:5729–5737. [PubMed: 21451108]
21. Veis DJ, Sentman CL, Bach EA, Korsmeyer SJ. Expression of the Bcl-2 protein in murine and human thymocytes and in peripheral T lymphocytes. J Immunol. 1993; 151:2546–2554. [PubMed: 8360476]
22. Dunkle A, Dzhagalov I, Gordy C, He YW. Transfer of CD8+ T cell memory using Bcl-2 as a marker. J Immunol. 2013; 190:940–947. [PubMed: 23269245]
23. Fischer K, Voelkl S, Berger J, Andreesen R, Pomorski T, Mackensen A. Antigen recognition induces phosphatidylserine exposure on the cell surface of human CD8+ T cells. Blood. 2006; 108:4094–4101. [PubMed: 16912227]
24. Williamson P, Christie A, Kohlin T, Schlegel RA, Comfurius P, Harmsma M, Zwaal RF, Bevers EM. Phospholipid scramblase activation pathways in lymphocytes. Biochemistry. 2001; 40:8065–8072. [PubMed: 11434775]
25. Chauhan SK, Saban DR, Lee HK, Dana R. Levels of Foxp3 in regulatory T cells reflect their functional status in transplantation. J Immunol. 2009; 182:148–153. [PubMed: 19109145]
26. Arandi N, Mirshafiey A, Abolhassani H, Jeddi-Tehrani M, Edalat R, Sadeghi B, Shaghaghi M, Aghamohammadi A. Frequency and expression of inhibitory markers of CD4(+) CD25(+) FOXP3(+) regulatory T cells in patients with common variable immunodeficiency. Scand J Immunol. 2013; 77:405–412. [PubMed: 23432692]
27. Venken K, Hellings N, Thewissen M, Somers V, Hensen K, Rummens JL, Medaer R, Hupperts R, Stinissen P. Compromised CD4+ CD25(high) regulatory T-cell function in patients with relapsing-remitting multiple sclerosis is correlated with a reduced frequency of FOXP3-positive cells and reduced FOXP3 expression at the single-cell level. Immunology. 2008; 123:79–89. [PubMed: 17897326]
28. Wang M, Windgassen D, Papoutsakis ET. A global transcriptional view of apoptosis in human T-cell activation. BMC Med Genomics. 2008; 1:53. [PubMed: 18947405]
29. Wang Z, Azmi AS, Ahmad A, Banerjee S, Wang S, Sarkar FH, Mohammad RM. TW-37, a small-molecule inhibitor of Bcl-2, inhibits cell growth and induces apoptosis in pancreatic cancer: involvement of Notch-1 signaling pathway. Cancer Res. 2009; 69:2757–2765. [PubMed: 19318573]
30. Akbar AN, Borthwick NJ, Wickremasinghe RG, Panayoitidis P, Pilling D, Bofill M, Krajewski S, Reed JC, Salmon M. Interleukin-2 receptor common gamma-chain signaling cytokines regulate activated T cell apoptosis in response to growth factor withdrawal: selective induction of anti-apoptotic (bcl-2, bcl-xL) but not pro-apoptotic (bax, bcl-xS) gene expression. Eur J Immunol. 1996; 26:294–299. [PubMed: 8617294]
31. Graninger WB, Steiner CW, Graninger MT, Aringer M, Smolen JS. Cytokine regulation of apoptosis and Bcl-2 expression in lymphocytes of patients with systemic lupus erythematosus. Cell Death Differ. 2000; 7:966–972. [PubMed: 11279543]

32. O'Brien SM, Claxton DF, Crump M, Faderl S, Kipps T, Keating MJ, Viallet J, Cheson BD. Phase I study of obatoclax mesylate (GX15-070), a small molecule pan-Bcl-2 family antagonist, in patients with advanced chronic lymphocytic leukemia. Blood. 2009; 113:299–305. [PubMed: 18931344]
33. Tai X, Van Laethem F, Pobezinsky L, Guinter T, Sharrow SO, Adams A, Granger L, Kruhlak M, Lindsten T, Thompson CB, Feigenbaum L, Singer A. Basis of CTLA-4 function in regulatory and conventional CD4(+) T cells. Blood. 2012; 119:5155–5163. [PubMed: 22403258]
34. Tang AL, Teijaro JR, Njau MN, Chandran SS, Azimzadeh A, Nadler SG, Rothstein DM, Farber DL. CTLA4 expression is an indicator and regulator of steady-state CD4+ FoxP3+ T cell homeostasis. J Immunol. 2008; 181:1806–1813. [PubMed: 18641318]
35. Wing K, Onishi Y, Prieto-Martin P, Yamaguchi T, Miyara M, Fehervari Z, Nomura T, Sakaguchi S. CTLA-4 control over Foxp3+ regulatory T cell function. Science. 2008; 322:271–275. [PubMed: 18845758]
36. Doi K, Li R, Sung SS, Wu H, Liu Y, Manieri W, Krishnegowda G, Awwad A, Dewey A, Liu X, Amin S, Cheng C, Qin Y, Schonbrunn E, Daughdrill G, Loughran TP Jr, Sebti S, Wang HG. Discovery of marinopyrrole A (maritoclax) as a selective Mcl-1 antagonist that overcomes ABT-737 resistance by binding to and targeting Mcl-1 for proteasomal degradation. J Biol Chem. 2012; 287:10224–10235. [PubMed: 22311987]
37. Russo M, Spagnuolo C, Volpe S, Tedesco I, Bilotto S, Russo GL. ABT-737 resistance in B-cells isolated from chronic lymphocytic leukemia patients and leukemia cell lines is overcome by the pleiotropic kinase inhibitor quercetin through Mcl-1 down-regulation. Biochem Pharmacol. 2013; 85:927–936. [PubMed: 23353698]
38. He L, Torres-Lockhart K, Forster N, Ramakrishnan S, Greninger P, Garnett MJ, McDermott U, Rothenberg SM, Benes CH, Ellisen LW. Mcl-1 and FBW7 control a dominant survival pathway underlying HDAC and Bcl-2 inhibitor synergy in squamous cell carcinoma. Cancer Discov. 2013; 3:324–337. [PubMed: 23274910]
39. Tang H, Shao H, Yu C, Hou J. Mcl-1 downregulation by YM155 contributes to its synergistic anti-tumor activities with ABT-263. Biochem Pharmacol. 2011; 82:1066–1072. [PubMed: 21784061]

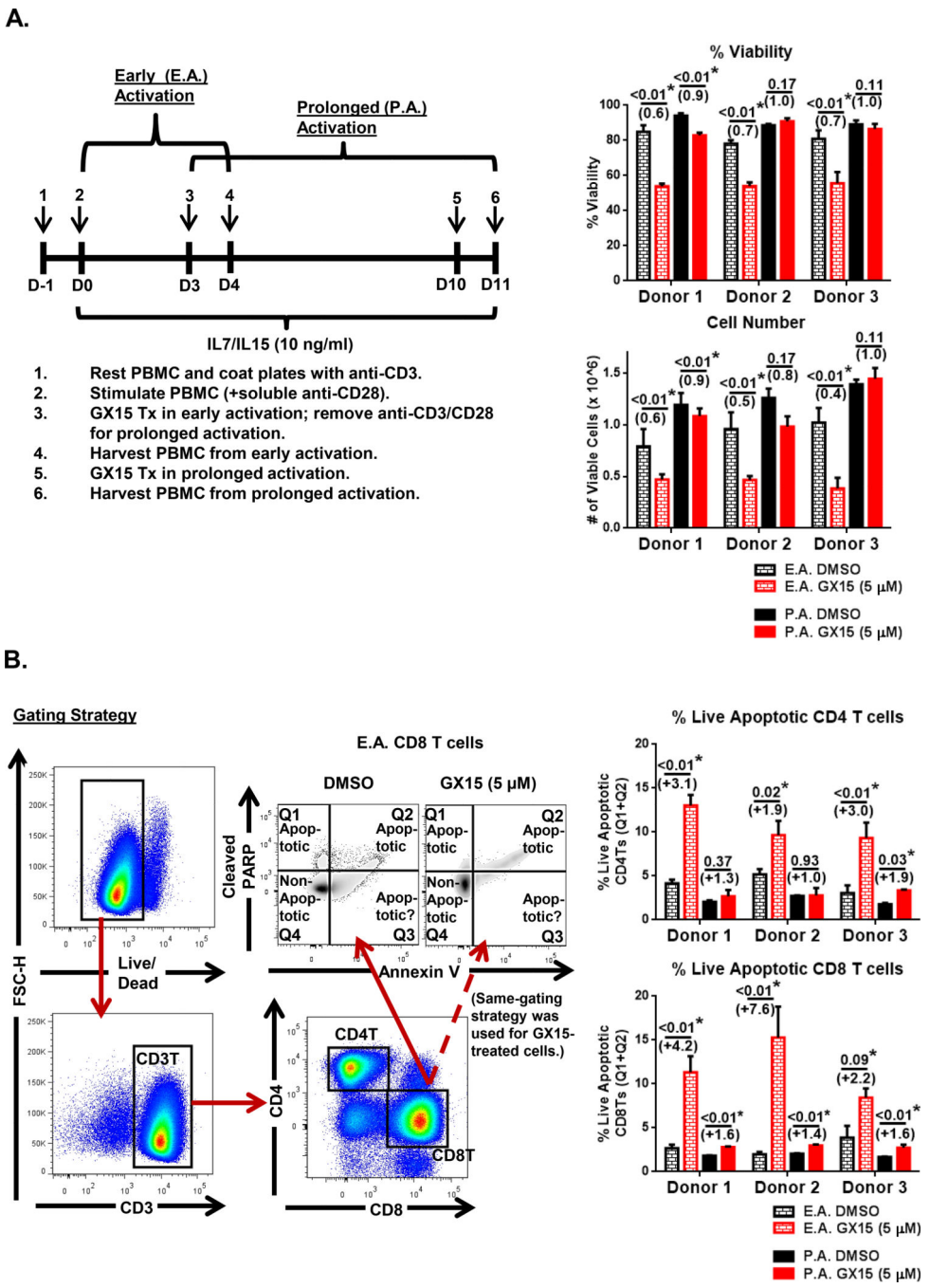

FIGURE 1.

CD4$^+$ and CD8$^+$ T cells from healthy-donor PBMCs were more sensitive to GX15 after early activation than after prolonged activation. **(A)** For early activation, healthy donor PBMCs were stimulated with anti-CD3 and anti-CD28 antibodies for 3 d, and then treated with GX15 for 24 h at 5 μM on day 3. For prolonged activation, early-activated PBMCs were supplemented on day 3 with IL-7 (10 ng/mL) and IL-15 (10 ng/mL) for an additional 7 d, and then treated with GX15 for 24 h at 5 μM on day 10. Bar graphs show the effect of GX15 on cell number and viability of PBMCs from 3 healthy donors after early and

prolonged activation, as measured by Trypan Blue exclusion. **(B)** The gating strategy to analyze percentages of early- and prolonged-activated $CD4^+$ and $CD8^+$ T cells undergoing apoptosis, as measured by cleaved PARP expression after GX15 treatment, is shown. Bar graphs show the apoptotic effect of GX15 on early- and prolonged-activated $CD4^+$ and $CD8^+$ T cells from 3 healthy donors. Error bars represent standard error of mean of triplicates. * indicates statistical significance ($p < 0.05$). The numbers in parentheses were calculated by dividing the GX15 group by the control group.

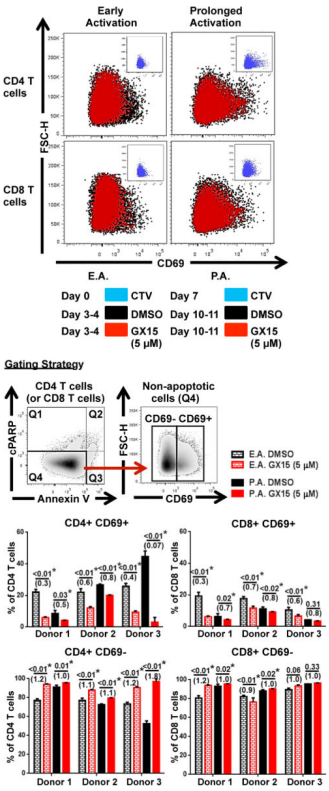

FIGURE 2.

Early-activated ($CD69^+$) T cells were more sensitive to GX15 than $CD69^-$ T cells after early and prolonged activation are shown. The gating strategy and representative flow cytometry analysis of the effect of GX15 on $CD69^+$ T cells after early and prolonged activation. Bar graphs indicate GX15-induced sensitivity of $CD69^+$ T cells from PBMCs of 3 healthy donors. Error bars represent standard error of mean of triplicates. * indicates statistical significance ($p < 0.05$). The numbers in parentheses were calculated by dividing the GX15 group by the control group.

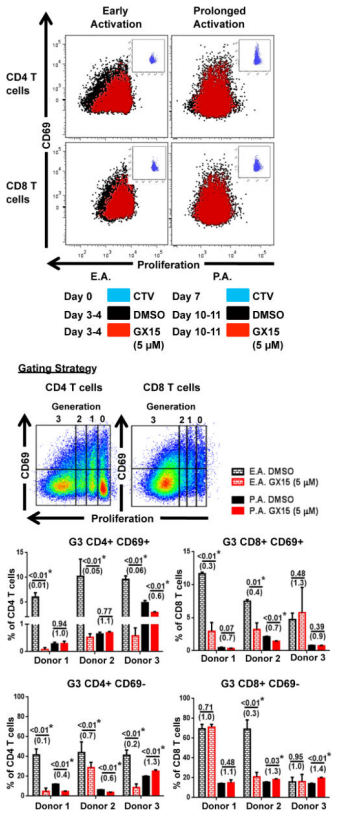

FIGURE 3.

Proliferation of early-activated ($CD69^+$) T cells was more sensitive to GX15 than that of $CD69^-$ T cells after early and prolonged activation. The gating strategy and representative proliferation analysis of CTV-labeled $CD69^+$ and $CD69^-$ T cells treated with GX15 (5 μM) after early and prolonged activation are shown. Bar graphs indicate the percentage of proliferating $CD69^+$ and $CD69^-$ T cells in Generation 3 after GX15 treatment. Error bars represent standard error of mean of triplicates. * indicates statistical significance ($p < 0.05$). The numbers in parentheses were calculated by dividing the GX15 group by the control group.

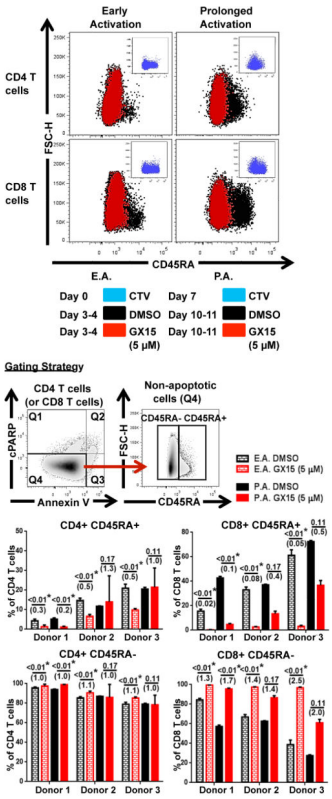

FIGURE 4.

Memory ($CD45RA^{-}$) T cells were resistant to GX15 after early and prolonged activation. The gating strategy and representative flow cytometry analysis of the effect of GX15 on non-memory ($CD45RA^{+}$) and memory ($CD45RA^{-}$) T cells after early and prolonged activation are shown. Bar graphs indicate GX15-induced sensitivity of $CD45RA^{+}$ and $CD45RA^{-}$ T cells from PBMCs of 3 healthy donors. Error bars represent standard error of mean of triplicates. * indicates statistical significance ($p < 0.05$). The numbers in parentheses were calculated by dividing the GX15 group by the control group.

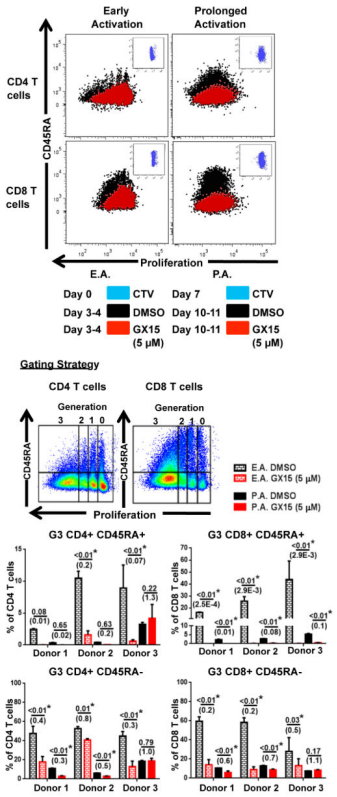

FIGURE 5.

Proliferation of non-memory ($CD45RA^+$)T cells was more sensitive to GX15 than that of memory ($CD45RA^-$) T cells after early and prolonged activation. The gating strategy and representative proliferation analysis of CTV-labeled $CD45RA^+$ and $CD45RA^-$ T cells treated with GX15 (5 μM) after early and prolonged activation are shown. Bar graphs indicate the percentage of proliferating $CD45RA^+$ and $CD45RA^-$ T cells in Generation 3 after GX15 treatment. Error bars represent standard error of mean of triplicates. * indicates statistical significance ($p < 0.05$). The numbers in parentheses were calculated by dividing the GX15 group by the control group.

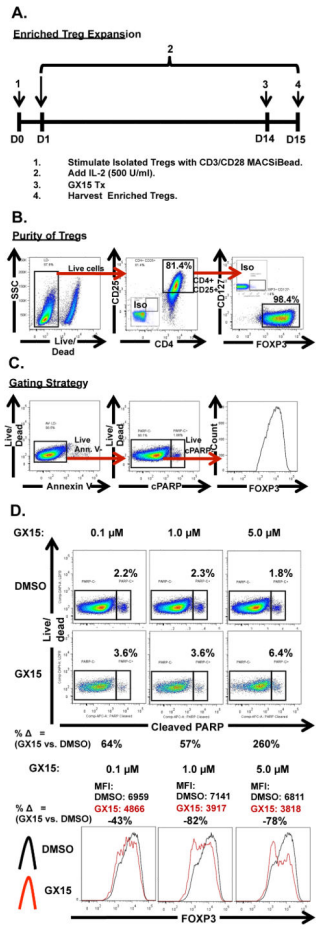

FIGURE 6.

GX15 increased apoptosis and induced down-regulation of FOXP3 on long-term expanded Tregs. (**A**) Schematic outline of enriched Treg expansion. After activation with CD3/CD28 beads, enriched Tregs were supplemented with IL-2 (500 U/mL) until day 14, when cells were treated with GX15 at 0.1, 1.0, and 5.0 μM. (**B**) Flow cytometry analysis of the purity of expanded Tregs. (**C**) Gating strategy for analysis of Tregs. (**D**) Effect of GX15 at 0.1, 1.0, and 5.0 μM on apoptosis of expanded Tregs. Percentages in the flow plots represent the proportion of live, annexin V^- Tregs that are positive for cleaved PARP (cPARP) expression. The percent change between GX15-treated and DMSO-treated Tregs at each concentration is also indicated. Histograms show the effect of GX15 at 0.1, 1.0, and 5 μM on FOXP3 expression in expanded Tregs. Black line indicates DMSO control-treated cells and red line indicates GX15-treated cells. Mean fluorescence intensity (MFI) of FOXP3 from GX15-treated or DMSO-treated Tregs at each concentration is also indicated.

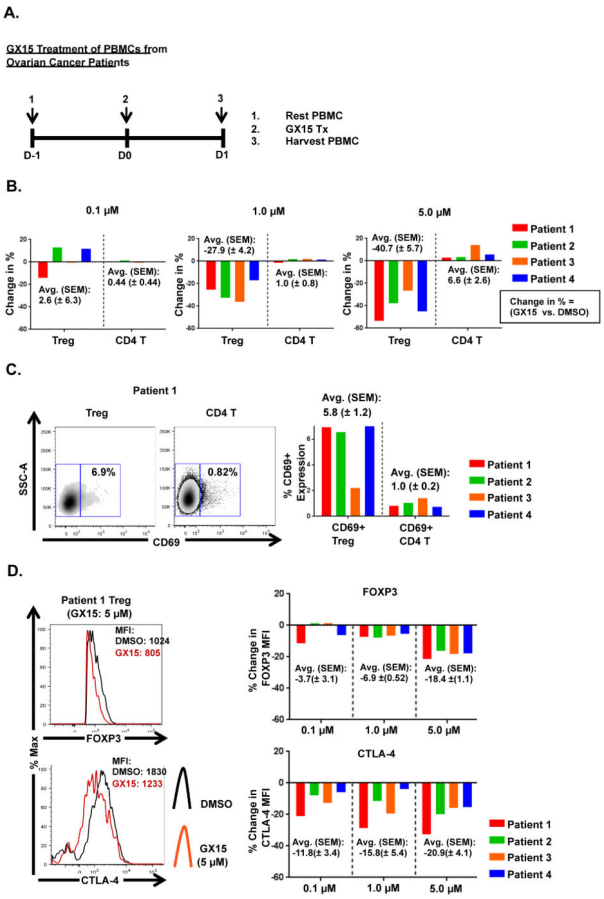

FIGURE 7.

Tregs were more sensitive than CD4$^+$ T cells to GX15. (**A**) Schematic outline of GX15 treatment of PBMCs from ovarian cancer patients (n = 4). PBMCs were rested 1 d prior to treatment and harvested 24 h post-treatment with GX15. (**B**) Bar graphs show the effect of GX15 at 0.1, 1.0, and 5.0 μM on Tregs and CD4$^+$ T cells. Change in % of Tregs or CD4$^+$ T cells was calculated as follows: For Tregs, [(%Treg $_{GX15}$-%Treg $_{DMSO}$)/%Treg $_{DMSO}$]x100. For CD4$^+$ T cells, [(%CD4$_{GX15}$- CD4$_{DMSO}$)/%CD4$_{DMSO}$]x100. Average and standard error of mean are also indicated. (**C**) Flow plots show percentages of Tregs and CD4$^+$ T cells expressing CD69. Bar graphs indicate average and standard error of mean. (**D**) Histograms show effect of GX15 on expression of FOXP3 and CTLA-4 in Tregs (red line: GX15 treatment; black line: DMSO control). Bar graphs indicate average and standard error of mean.

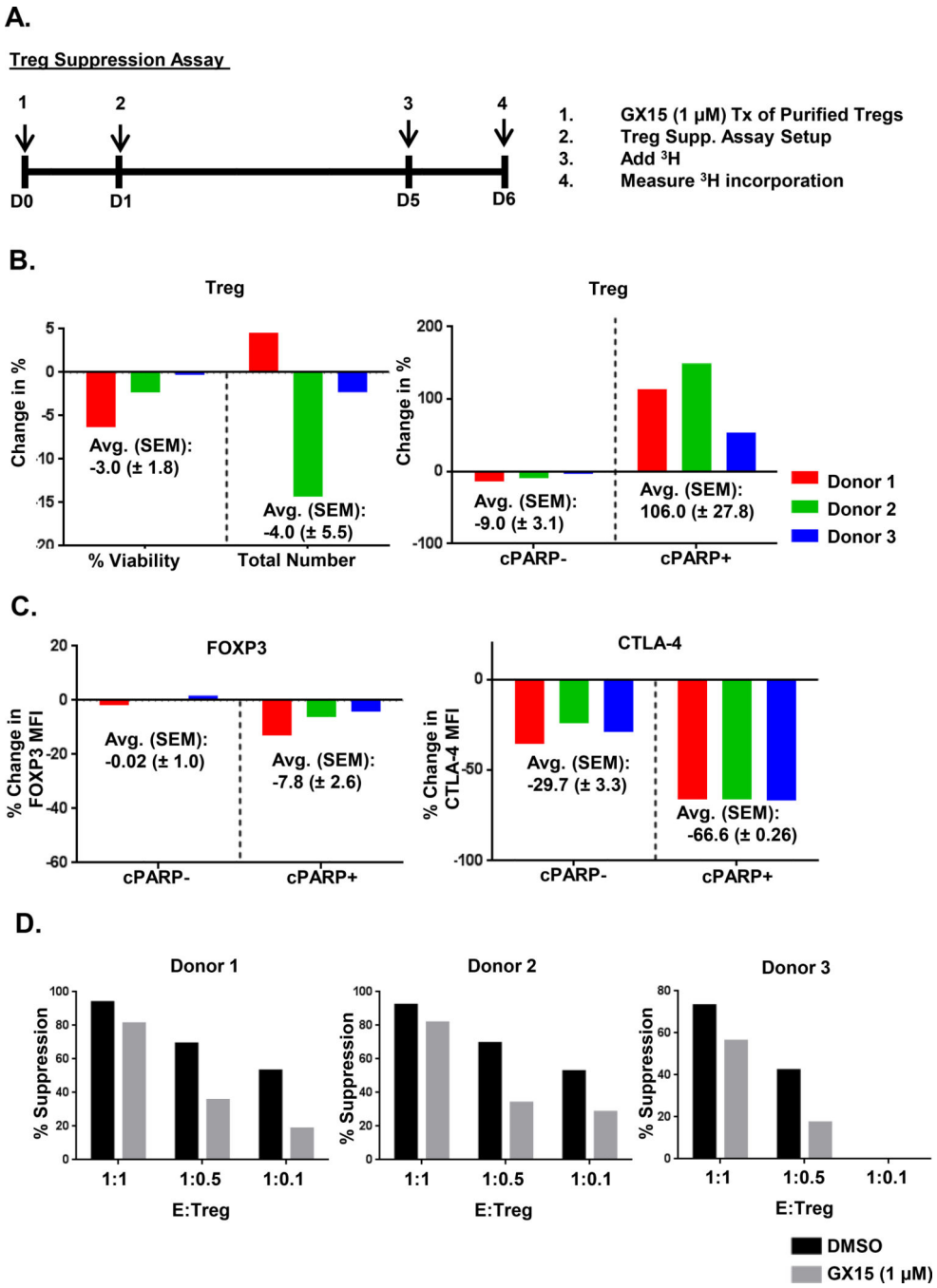

FIGURE 8.

The suppressive activity of Tregs is reduced after GX15 treatment. **(A)** Schematic outline of GX15 treatment of Tregs isolated from normal donor PBMCs (n=3). Purified Tregs were treated with 1.0 μM of GX15 for 24 h after which GX15-treated Tregs were washed, and then co-cultured with conventional $CD4^+$ T cells for 4 d after which ^3H was added for 24 h and then its incorporation was measured. **(B)** Bar graphs indicate the % change in viability and cell number and in cleaved PARP (cPARP) after GX15 treatment at 1.0 μM. Average and standard error of mean of the % change are also shown. **(C)** Bar graphs show the %

change in mean fluorescence intensity (MFI) of FOXP3 and CTLA4 in cPARP^{+} and cPARP^{-} Tregs. Average and standard error of mean of the % change are also shown. **(D)** Bar graphs indicate the suppressive activity of GX15-treated Tregs at various effector:Treg ratios.

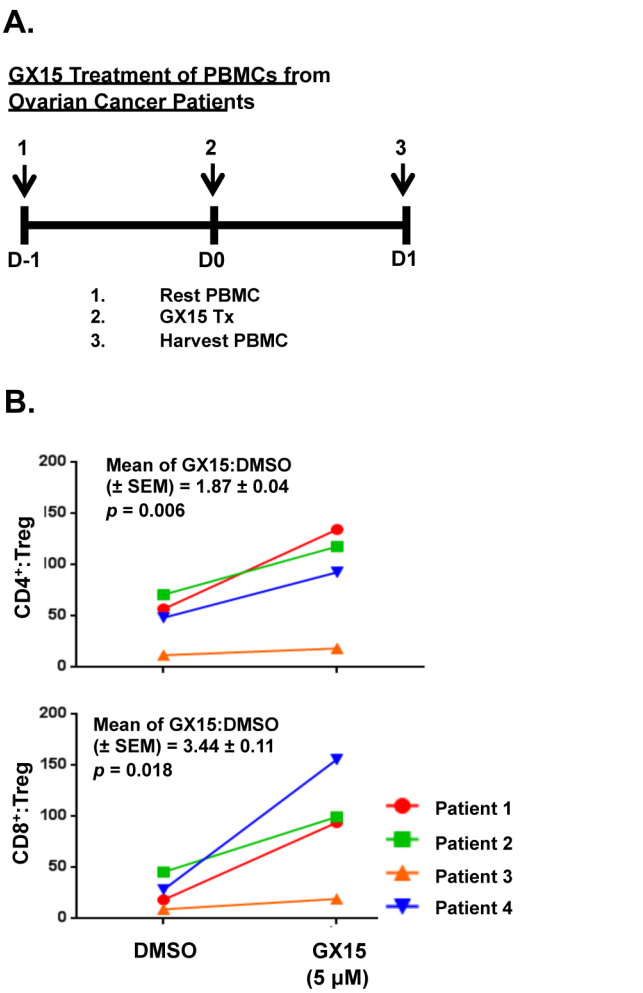

CD4⁺:Treg	No.	%
Increased	3/4	75%
Unchanged	1/4	25%
Decreased	0/4	0%

CD8⁺:Treg	No.	%
Increased	3/4	75%
Unchanged	1/4	25%
Decreased	0/4	0%

FIGURE 9.

In PBMCs from ovarian cancer patients, $CD4^+$:Treg and $CD8^+$:Treg ratios increased after *in vitro* treatment with GX15. (**A**) Schematic outline of GX15 treatment of PBMCs from ovarian cancer patients (as described in Fig. 7A). (**B**) Graphs show changes in the $CD4^+$:Treg and $CD8^+$:Treg ratios in PBMCs from ovarian cancer patients after treatment with GX15. The $CD4^+$:Treg and $CD8^+$:Treg ratios were calculated using the percentage of non-Treg $CD4^+$ T cells or $CD8^+$ T cells and the percentage of Tregs after treatment with GX15 or control. Means and standard error of means are indicated. Tables show the number and percentage of patients whose $CD4^+$:Treg and $CD8^+$:Treg ratios increased (> +20%), decreased (< −20%) or remained unchanged (< +20% and > −20%) after GX15 treatment.